

# Nonlinear control for buck switching power supplies using opto-couplers in the stabilization feedback loop

N. BIZON\*, E. SOFRON, M. RADUCU, M. OPROESCU  
University of Pitesti, Pitesti, Romania

Buck switching power supplies usually use a PWM voltage control to stabilize the output voltage at the reference voltage level. If a classical PWM control technique is used, than high EMI noise peaks appear at the switching frequency and its harmonics. Spreading of the output voltage spectrum can be done, for example, by chaotification of the PWM command signal. This kind of the switching power supplies with low EMI is utilize in electronics equipments from different domains: medical, aeronautics etc. The proposed nonlinear control is based on the opto-coupler nonlinear characteristic included into nonlinear circuit of the feedback loop. The feedback nonlinear circuit assures a symmetrical nonlinear characteristic using two opto-couplers and a differential amplifier. The nonlinear characteristic is designed to minimize output voltage ripple. The nonlinear characteristic is initially modeled by a look-up table for an easy designing by changing of the characteristic parameters using trial and error method. The feasibility and effectiveness of this new and relative simple method is shown by simulation.

(Received July 27, 2009; accepted June 16, 2010)

**Keywords:** PWM voltage control, Switching power supplies, Nonlinear control, Opto-coupler, Chaotification, Spread power spectrum, Output voltage ripple

## 1. Introduction

The buck converter is a DC-DC converter used to obtain a stabilized output voltage from a given input DC voltage which is lower than input voltage using switching techniques and Pulse Width Modulation (PWM) control method [1-4]. PWM voltage control is usually used to control the buck output voltage at the reference voltage level (Fig. 1).

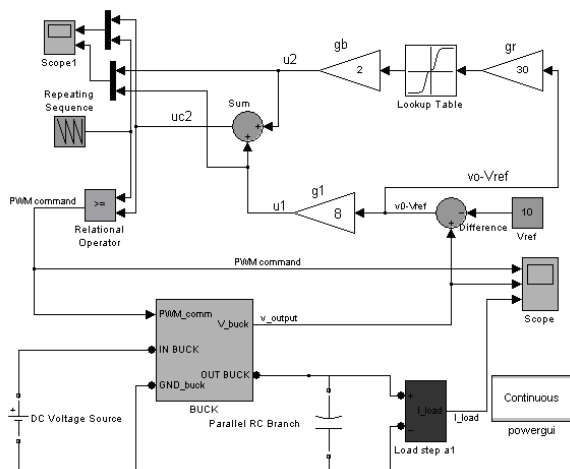


Fig. 1. Proposed nonlinear control loop.

The imposed output voltage ripple can be obtained by filtering the output voltage through an appropriate capacitor. The classical feedback produces  $u1$  feedback signal:

$$v_{cl}(t) = u1(t) = g_1 \cdot (v_o(t) - V_{ref}),$$

where  $g_1$  is a gain factor.

The  $v_{cl}(t)$  voltage is compared with saw-tooth voltage in order to obtain the PWM command for the IGBT switch (Fig. 2). The saw-tooth voltage,  $v_r(t)$ , is defined by relation:

$$v_r(t) = V_L + (V_H - V_L) \cdot \frac{t(\text{mod } T)}{T}$$

and is a decreasing ramp voltage from a higher voltage  $V_H$  to an lower voltage  $V_L$  in a switching time  $T$ .

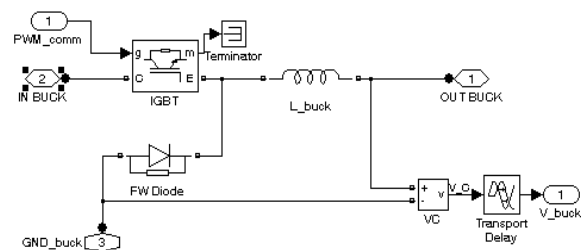


Fig. 2. Buck converter structure.

In the stabilized regime  $|v_{cl}(t)| \ll (V_H - V_L)$  and the buck converter operate at a fixed switching frequency, so high peak of the output power spectrum appear at the switching frequency  $f=1/T$  and its harmonics, generating high electromagnetic interference (EMI) [5-9]. Different

methods are proposed to change the switching frequency in order to spreading output power [10-17].

In this paper we propose an improved control technique, based on adding a feedback signal  $u_2(t)$ :

$$v_{c2}(t) = u_1(t) + u_2(t),$$

where  $u_2(t)$  feedback signal has two gain parameters:  $g_r$  fix the maximum output voltage ripple and  $g_b$  is chosen as bifurcation parameters.

Proposed control method is of bang-bang type and clearly is totally different by classical PWM control method: here the saw-tooth voltage has role of the chaotifying function for buck behavior. That new control method improves the EMI and minimize output voltage ripple. In this paper the nonlinear feedback controller characteristic is tested and designed for using in isolated switching power supplies, so the opto-coupler nonlinear characteristic is considered for practical implementation. The simulation results shows that, in comparison with the classical PWM control method, the nonlinear controller provides almost the same good voltage stabilization but with better dynamic response, robustness against system uncertainty disturbances and load pulses, and an implicit stability proof. The EMI level is low by spreading of the output power spectrum in large frequencies band, and output voltage ripple is minimize by a proper designing of the feedback nonlinear characteristic.

The paper is organized in five sections, and first section was this introduction. In order to understand how to operate the nonlinear feedback control, in the second sections this are briefly explained using a look-up table. The influence of the nonlinear characteristic parameters and circuit parameters are estimated by simulation (the basic test set is:  $L=20\text{mH}$ ,  $C=47\mu\text{F}$ ,  $R=22\Omega$ ,  $V_{ref}=10\text{V}$ ,  $V_L=4\text{V}$ ,  $V_H=8\text{V}$ ,  $T=400\mu\text{s}$ ,  $g_l=8$ ,  $g_r=30$ ,  $g_b=2$ , and DC input source,  $E = 20\text{V}$ ). The optimized nonlinear feedback control is implemented in next section using a differential amplifier that combine the nonlinear characteristic of two opto-couplers and a summing amplifier of the feedback signals,  $u_1(t)$  and  $u_2(t)$ . Simulation and experimental results for a buck converter with this proposed feedback loop circuits are presented in the last section (using Matlab and Spice @simulators), and finally some conclusions are given.

## 2. Designing and modeling the feedback nonlinear control circuit

The used basic test set is:  $L=20\text{mH}$ ,  $C=47\mu\text{F}$ ,  $R=22\Omega$ ,  $V_{ref}=10\text{V}$ ,  $V_L=4\text{V}$ ,  $V_H=8\text{V}$ ,  $T=400\mu\text{s}$ ,  $g_l=8$ ,  $g_r=30$ ,  $g_b=2$ , and DC source,  $E = 20\text{V}$ . When a parameter value is changed that will be mention in every situation. The parameter sensitivity and influence on the control performances was estimated by simulation for all circuit parameters. Some design relations concerning the relations between the nonlinear characteristic parameters and circuit performances were obtained by trial and error method.

First nonlinear characteristic is implemented by a look-up table and use in simulation following vectors (the vectors values are done in volts; see Fig. 3):

Input vector:

$[-1, -0.6, -0.4, -0.3, -0.15, 0.15, 0.3, 0.4, 0.6, 1]$ ;

Output vector:  $[-5, -5, -4.7, -4, -0.5, 0.5, 4, 4.7, 5, 5]$ .

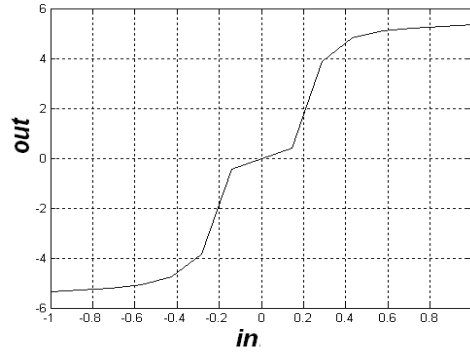


Fig. 3. Nonlinear transfer characteristic implemented by a look-up table

This look-up table approximates the control law of a fuzzy logic controller that uses a rules base which minimizes the output voltage ripple [18].

For  $v_{c2}$  control law the output power spectrum is less sensitive to  $g_l$  gain parameter: for a low  $g_l$  gain (figure 4 - top) the spectrum spreading band is a little bit higher than for high  $g_l$  gain (Fig. 4 - bottom).

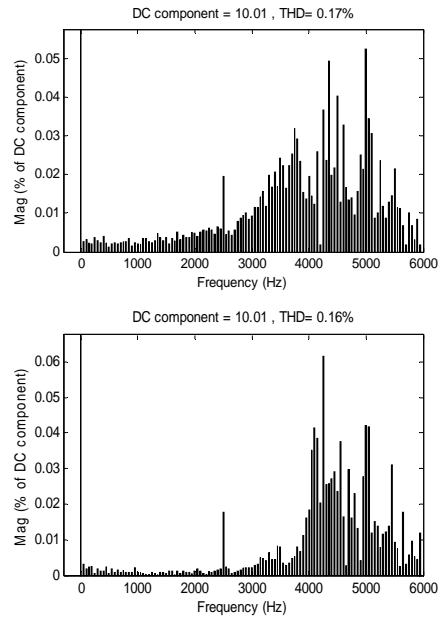


Fig. 4. Output power spectrum for  $v_{c2}$  control law with basic parameters using different  $g_l$  gain values:  $g_l=4$  (top);  $g_l=16$  (bottom).

The output voltage ripple remains almost the same for different  $g_1$  gain values in range 4 to 16.

The position of the output power spectrum can be modified by choosing the output filter capacity value. For a high filter capacity the output power spectrum is concentrate in the low frequencies band (Fig. 5 - top) and for a low filter capacity the output power spectrum is moved to the high frequencies band (Fig. 5 - down).

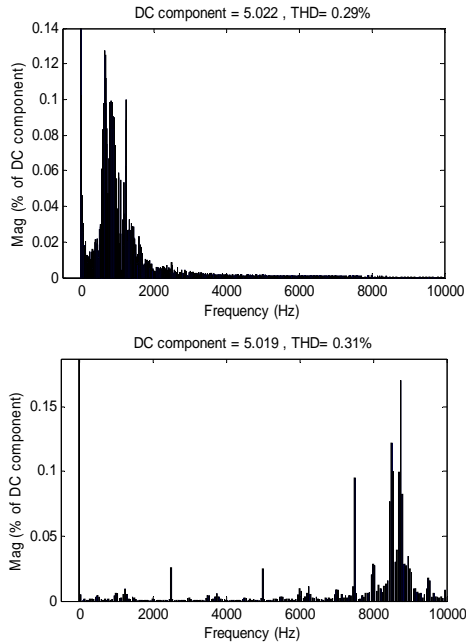


Fig. 5. Output voltage spectrum for different  $C$  values:  $C=470\mu\text{F}$  (top);  $C=4.7\mu\text{F}$  (bottom).

The output voltage ripple remains almost the same for  $v_{c2}$  control law with basic parameters using different output filter capacity values in range  $4.7\mu\text{F}$  to  $470\mu\text{F}$  because that is more dependent by  $g_r$  ripple gain.

A low  $g_r$  ripple gain gives a high ripple output voltage and the output power spectrum is concentrate at low frequencies. A high  $g_r$  ripple gain gives a low ripple output voltage, but not smaller than a limit (about  $\Delta v_{o(p-p)\min} = 40\text{mV}$  for basic test set) and the output power spectrum is more concentrate around of a frequency (about 4kHz for basic test set).

The saw-tooth voltage parameters,  $V_H$  and  $V_L$ , must be designed in correlation with output range of the nonlinear characteristic (output vector of the look-up table).

For a simple look-up table (as represented in Fig. 3) which are:

Input vector:  $[-t, -p, -q, q, p, t]$ , where  $t=1$ ;  $p=0.6$ ;  $q=0.15$ ;

Output vector:  $[-r, -r, -s, s, r, r]$ , where  $r=5$ ;  $s=0.5$ , the gain in different input zones are:

a) In the inner gain zone  $[-q, q]$ , for input  $x \in [-q, q]$  the gain is  $\frac{s}{q} \cdot x$ ;

b) In the variable gain zone  $[-p, -q]$  and  $[q, p]$ , for input  $x \in [q, p]$  the gain is  $\frac{r-s}{p-q}(x-q) + s$ ;

c) In the limited gain zone  $[-r, -p]$  and  $[r, p]$ , for input  $x \in [q, p]$  the gain is  $r$ .

If we choose

$$r \cdot g_b > V_H \text{ and } s \cdot g_b < V_L$$

the system performance regarding the output power spectrum spreading remain almost the same.

The output voltage ripple,  $\Delta v_{o(p-p)}$ , can be limited at imposed range,  $\Delta v_{o(p-p)\min}$  to  $\Delta v_{o(p-p)\max}$ , choosing:

$$\Delta v_{o(p-p)\min} \cdot g_r \approx q \text{ and } \Delta v_{o(p-p)\max} \cdot g_r \approx p.$$

The saw-tooth voltage frequency  $f=1/T$  and output filter frequency,  $f_{RC} = \frac{1}{2\pi \cdot R \cdot C}$ , where  $C$  is filter capacity and  $R$  is the load, must be in relation  $0.03 \cdot f < f_{RC} < f$  to assure a good spreading of the output power spectrum. For basic test set results  $f = 2.5$  kHz and  $f_i \approx 1$  kHz. The load can have a large range for variation: from  $5\Omega$  ( $f_i \approx 4.255$  kHz) to  $30\Omega$  ( $f_i \approx 0.7$  kHz). For a given load in middle range the filter capacity can have a large range for variation, too (see Fig. 6).

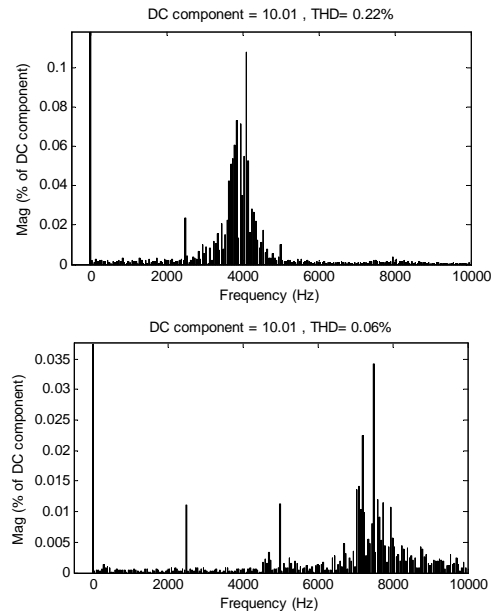


Fig. 6. Output voltage spectrum for different  $C$  values:  $C=470\mu\text{F}$  (top);  $C=4.7\mu\text{F}$  (bottom).

### 3. Implementation of the feedback nonlinear circuit

There are many ways to implement a nonlinear circuit [18,19]. In this case the restrictions are: the electrical isolation between command part and input/output power part; simple implementation etc. To assure the first restriction, all proposed switching power supplies assure the electrical isolation for power flow between input power part and output power part by a transformer, and, usually, for feedback signal from output power part to command part by a circuit with opto-coupler. For the PWM control method the opto-coupler operate in the quasi-linear zone of opto-coupler characteristic with small feedback signal as input signal. For an improved dynamic in the feedback loop is inserted a tuned Proportional-Integrator (PI) controller. The electrical isolation of the feedback signal can be made before or after the PI controller. The output signal of the PI controller is compared with saw-tooth signal in order to obtain the switching command signal (Fig. 7).

For the proposed control method the feedback signal is output error voltage gained by two gain constants ( $g_r$  and  $g_b$ ) and one variable gain (given by nonlinear characteristic function of output voltage ripple). The feedback signal is higher that classical PWM control case (comparable at peak to peak level with saw-tooth signal), so the switching times are dependent by loop global gain and saw-tooth signal parameters (chosen as chaotizing function for its simplicity in implementation).

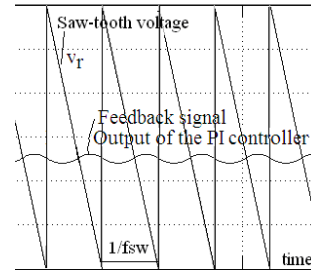


Fig. 7. PWM principle.

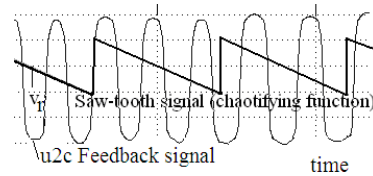


Fig. 8. Proposed switching principle.

The shape of the chaotizing function isn't too important, but its periodicity must be correlated with buck time constants, which give the associate frequencies:

$$f_{LC} = 1/2\pi\sqrt{LC}, f_{RC} = 1/2\pi RC, f_{LR} = R/2\pi L$$

More important, but not critical, is the shape of the nonlinear characteristic, given by designing relations of the knee points, (p, r) and (q, s), in above section.

To obtain a symmetrical characteristic like as presented in Fig. 3, two isolated channel are used. Last stage summing the channels output signals (Fig. 9).

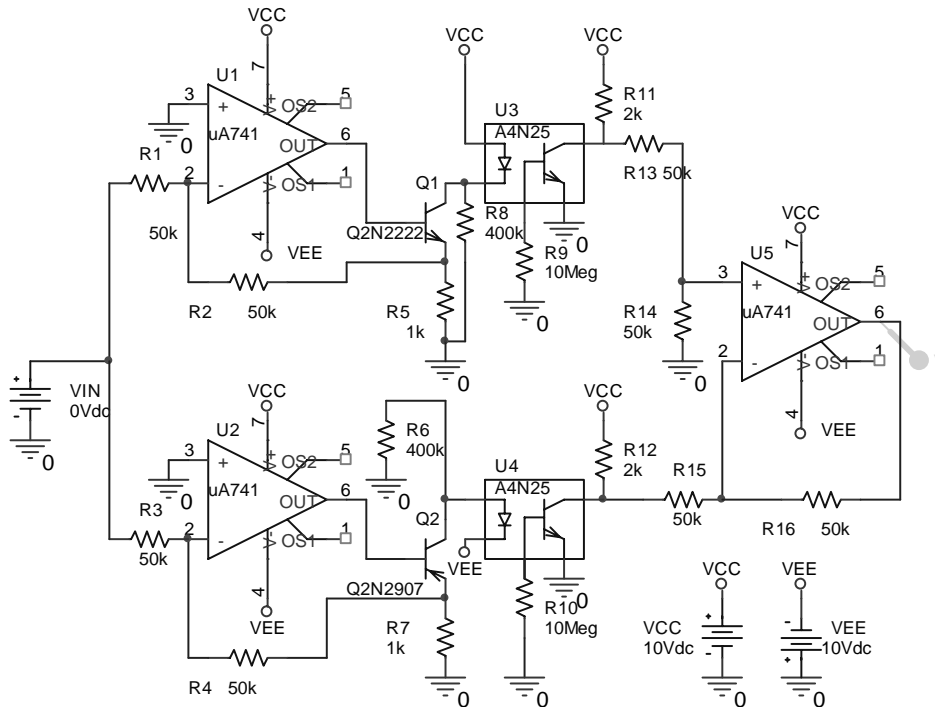
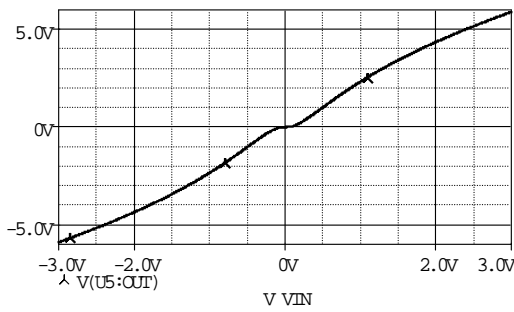
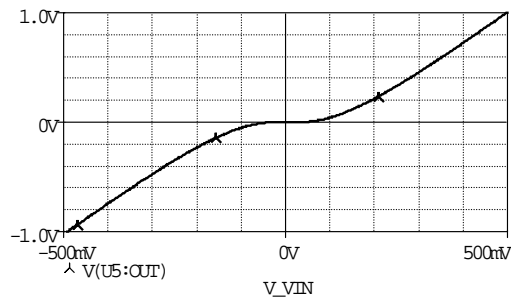


Fig. 9. Feedback nonlinear circuit.

The resulting transfer characteristic of the nonlinear circuit from Fig. 9 is presented in Fig. 10.



(a)



(b)

Fig. 10.a. Transfer characteristic of the nonlinear circuit; (b) A zoom of the transfer characteristic in the inner zone.

More sophisticated implementations of the nonlinear circuit can be imagined, but this simple implementation can assure well results both in the frequency-domain (power spectrum spreading) and in the time-domain (output voltage ripple minimization). The feasibility and usefulness of this quite simple control method is shown by simulation for a buck converter in the next section.

#### 4. Simulation results

The complete Spice diagram of the buck converter, with proposed nonlinear control loop as in Fig. 1, is shown in Fig. 11. The same values are used for basic test:  $L=20\text{mH}$ ,  $C=47\mu\text{F}$ ,  $R=22\Omega$ ,  $V_{ref}=10\text{V}$ ,  $V_L=4\text{V}$ ,  $V_H=8\text{V}$ ,  $T=400\mu\text{s}$ ,  $g_I=8$ . The new designed parameters are:  $g_r=4$ ,  $g_b=20$ . In both case (Matlab and Spice simulation) we set  $g_1=0$  in order to see if the nonlinear loop can only assure the buck control.

Fig. 12 show in the top plot the feedback and the saw-tooth signals, and in bottom plot the output voltage. The signals shapes lock as the same signals shape in Matlab simulation (see Fig. 8). Another time zoom of the output voltage is presented in Fig. 13 (top plot) and compared as shape with Matlab simulation of the output voltage error (bottom plot).

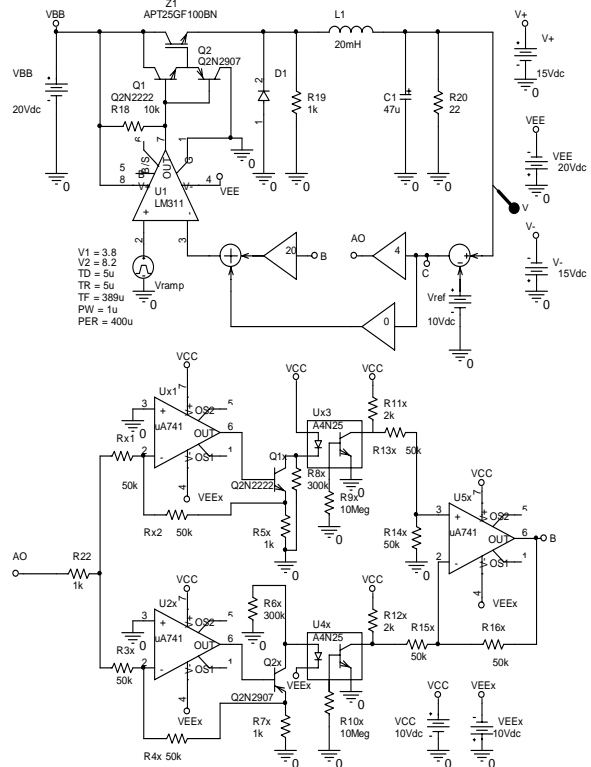


Fig. 11. Spice diagram of the buck converter with proposed nonlinear control loop as in Fig. 1.

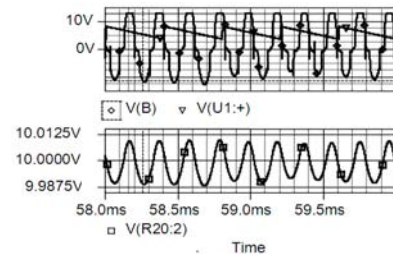


Fig. 12. Spice simulation results for buck converter.

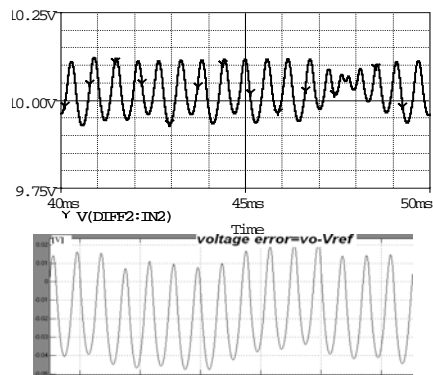


Fig. 13. Output voltage (Spice simulation – top; Matlab simulation – bottom).

Output voltage spectrum using Spice simulation is shown in Fig. 14, and this lock as shape and spreading

band with output voltage spectrum using Matlab simulation (see Figs. 4, 5, and 15).

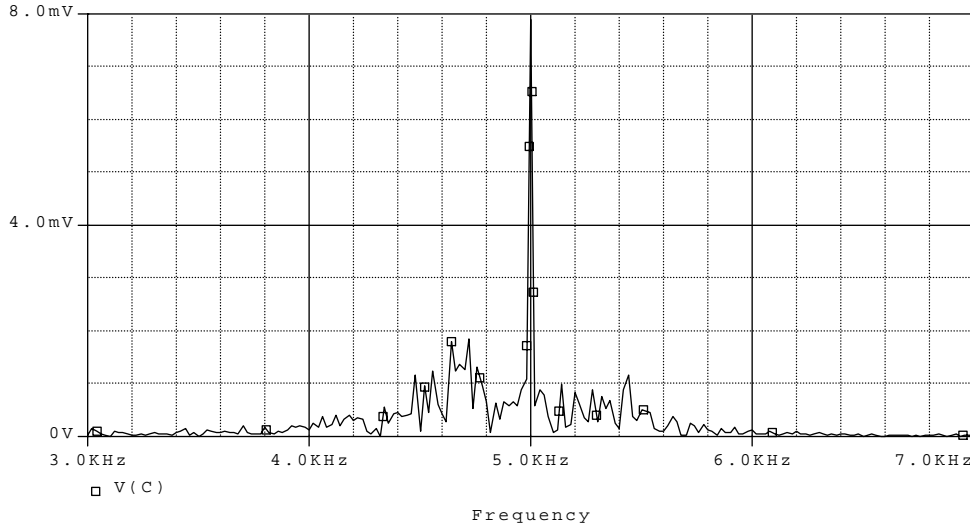


Fig.14. Output voltage spectrum using Spice simulation.

The output voltage spectrums are represented in Fig. 15 for control law  $v_{c2}$  with  $g_r=2$ ,  $g_b=30$ ,  $C=47\mu F$  and  $V_{ref}=10V$ , using different  $g_1$  gain: 0 (top); 10 (middle); 20 (bottom). Power spectrum spreading can be measured by two performance indexes:

$$\frac{\Delta f_{10\%}}{f_{COG}} \text{ and } \frac{THD}{S_{peak}}$$

where

- $S_{peak}$  is the maximum spectral magnitude (% of DC component),
- $\Delta f_{10\%}$  is the frequencies band where (spectral magnitude)/ $S_{peak} > 10\%$ ,
- $f_{COG}$  is the frequency that is center of gravity of the power spectrum, and
- THD is total harmonics distortion coefficient for output error voltage.

The THD parameter is a measure of output voltage ripple (Fig. 16), too. Analyzing Fig. 15 we can conclude that spreading of the output voltage spectrum and output voltage ripple are less sensitive to  $g_1$  gain. This can simplify the control loop circuit: the amplifier with gain  $g_1=0$  can miss.

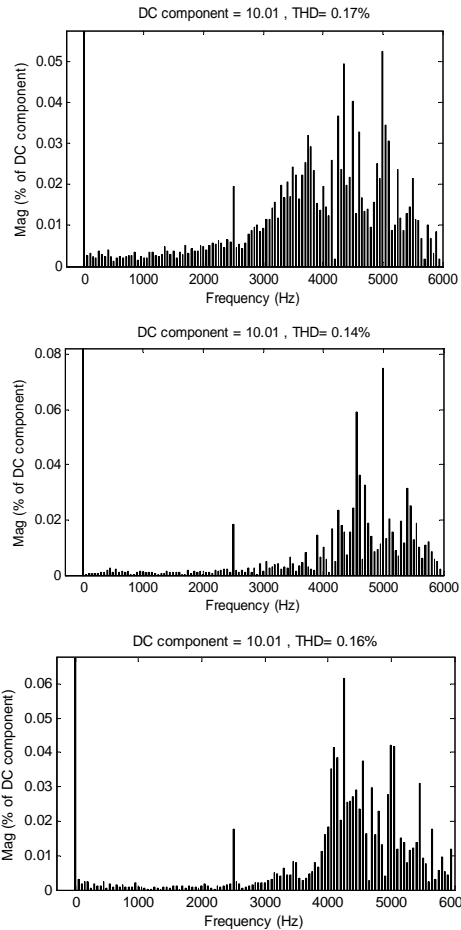


Fig. 15. Output voltage spectrum for control law  $v_{c2}$  with  $g_4=2$ ,  $g_5=30$ , and  $V_{ref}=10V$ , using different  $g_1$  gains: 0 (top); 10 (middle); 20 (bottom).

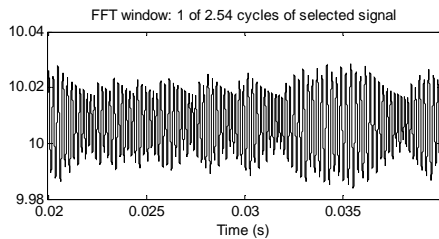


Fig. 16. Output voltage ripple.

## 5. Conclusions

The proposed nonlinear controller based on opto-coupler characteristic nonlinearity is quite simple and designing parameters are not strictly. The opto-coupler nonlinearity is used in feedback signal processing in order to minimize the output voltage ripple.

Spreading of the power spectrum is obtained by a chaotizing function: a saw-tooth generator in this paper. An explanation of the proposed control proprieties is the increase of feedback signal frequency in nonlinear closed loop in order to maintain a small voltage ripple. Some design rules are obtained by a rigorous analysis of the many study cases.

Applying the proposed control method to switch-mode power converter improves the performance both in the frequency-domain (spectrum) and in the time-domain (ripple). The control performances are shown by Matlab simulation, and practical implementation is tested with Spice. The simulation results are almost the same as shape, and performance indices evaluation, respectively.

## Acknowledgments

The CNCSIS Grant #570 of the National Research Council (MEC) has supported part of the research.

## References

[1] I. Batarseh, Power electronic circuits, Hoboken, NJ: John Wiley, 2004.

- [2] N. Bizon, Power converters (in romanian language), Ed. MatrixROM, Bucharest, 2004.
- [3] J. P. Agrawal, Power electronic systems: theory and design, Upper Saddle River, N.J.: Prentice Hall, 2001.
- [4] M. H. Rashid, Power Electronics: Circuits, Devices and Applications (3rd Edition), Prentice Hall, 2003.
- [5] A. Mogel, J. Krupar, W. Schwarz, EMI performance of spread spectrum clock signals with respect to the IF bandwidth of the EMC standard, Proceedings of the 2005 European Conference on Circuit Theory and Design, **1**, 1/169 (2005).
- [6] Yang, Ken, Spread-Spectrum DC-DC Converter Combats EMI, Electronic Design, 86, 2001.
- [7] H. Li, B. Zhang, Proc. 16th China Power Supply Society Conf., 605, 2005.
- [8] S. Banerjee, D. Kastha, S. SenGupta, Proceedings of the International Conference on Electromagnetic Interference and Compatibility, 162, 2002.
- [9] H. Wong, Y. Chan, S. W. Ma, 23rd International Conference on Microelectronics - MIEL 2002, **2**, 577 (2002).
- [10] A. M. Stankovic, G. C. Verghese, D. J. Perreault, IEEE Trans. on Power Electronics **10**(6), 680 (1995).
- [11] K. K. Tse, R. W. M. Ng, H. S. H. Chung, et al., IEEE Trans. on Industrial Electronics **50**(1), 171 (2003).
- [12] M. Kuisma, Systems Magazine **18**(12), 18 (2003).
- [13] C. Morel, M. Bourcier, F. Chapeau-Blondeau, Journal of Circuits, Systems, and Computers **14**(4), 757 (2005).
- [14] C. Morel, M. Bourcier, F. Chapeau-Blondeau, Proc. IEEE Int. Symp. Industrial Electronics ISIE'04, 447, 2004.
- [15] X. F. Wang, G. Chen, Int. J. Circuit Theor. Appl. **28**, 305 (2000).
- [16] Z-Z. Li, S-S. Qiu, Y-F. Chen, Proceedings of the Chinese society for electrical engineering **26**(5), 76 (2006).
- [17] N. Bizon, Simulation and System's Identification SIMSIS 2007, proceedings on CD (2007).
- [18] N. Bizon, Chaotification of the buck converter using a modified Chua's diode, Fuzzy Systems and AI journal - Reports and Letters (in press).
- [19] M. P. Kennedy, Frequenz **46**(3-4), 66 (1998).

\*Corresponding author: nicubizon@yahoo.com